Automating a Spatial Profiling Workflow To Explore The Effects Of Hypoxia In The Tumor Microenvironment In Head And Neck Cancer

[1] Kelly Hunter , [1] Joana Campos , [1] Jack L. McMurray, [1] Melanie Weigand, [1] Chris Morse, [1] Ketaki Hardikar, [2] Jeni Caldara,[2] Regan Baird,[2] David Mason,[3] Kyla Teplitz,[2]James Mansfield,[4] Hisham Mehanna,[4] Jill Brooks

[1] Propath, Hereford, UK, [2] Visiopharm, Horsholm, Denmark, [3] Bruker, Seattle, WA, USA, [4] Institute of Head and Neck Studies and Education, University of Birmingham, Birmingham, UK

Abstract

Background: Head and neck cancer (HNC) is a heterogeneous group of malignancies that arise from the mucosal surfaces of the upper aerodigestive tract. The tumor microenvironment (TME) of HNC is characterized by the presence of immune cells, stromal cells, and extracellular matrix components. A key feature of the TME is hypoxia, which promotes tumor growth, invasion, and metastasis by altering the expression of genes involved in angiogenesis, cell survival, and metabolism. Understanding the complex interplay between hypoxia and immune infiltrates in the TME of HNC is crucial for the development of novel therapeutic strategies for the treatment of this disease. Whole transcriptome analysis by digital spatial profiling is an excellent method of probing the TME, but assessing large cohorts can be time consuming. Automating a profiling workflow to reduce hands-on time and region of interest (ROI) selection bias will enable exploration of large cohorts to identify mechanisms of action, potential drug targets, and biomarkers.

Methods: We developed an optimized spatial multi-omic workflow to enable high-throughput spatial analysis on GeoMx® Digital Spatial Profiler (DSP) using the Whole Transcriptome Atlas (WTA) and immuno-fluorescent morphology markers: SYTO82 (nuclei), CAIX (hypoxia), pan-cytokeratin (epithelium), CD3 (T-cells). A.I.-based analysis (Oncotopix® Discovery) of serial section H&E images and GeoMx IF images was developed to identify ROIs for GeoMx collection. Immune hot and cold selection used leukocyte density; tumor/stromal interface selection used epithelial areas. Areas of illumination (AOI) were chosen using concentric CAIX expression gradients. Integrated analysis of digital images using Oncotopix Discovery and the whole transcriptome was done to assess the above TME compartments.

Results: Automated ROI placement based on tumor/stroma, hypoxia and immune infiltration and AI /Deep Learning based AOI segmentation reduced AOI selection time and improved accuracy of tissue compartment enrichment, especially between samples and tissue types. Automated development of hypoxia gradient-based AOI enabled a selection strategy not possible in the standard DSP software. Cell phenotyping using IF morphology scan was used to supervise cell deconvolution. DSP results correlated well with patient outcomes.

Conclusions: This work shows that ROI-based spatial analyses can be used to explore the effects of hypoxia levels on immune infiltration in HNC. Automated AI-based ROI selection provides a means of sampling relevant tumor subtypes based on hypoxia and immune infiltrate criteria in an unbiased, reproducible manner, and can provide a standardized, automated method for selecting ROIs and segmenting AOIs across a cohort of mixed tissue types and pathological subtype, improving throughput

ROI & AOI selection

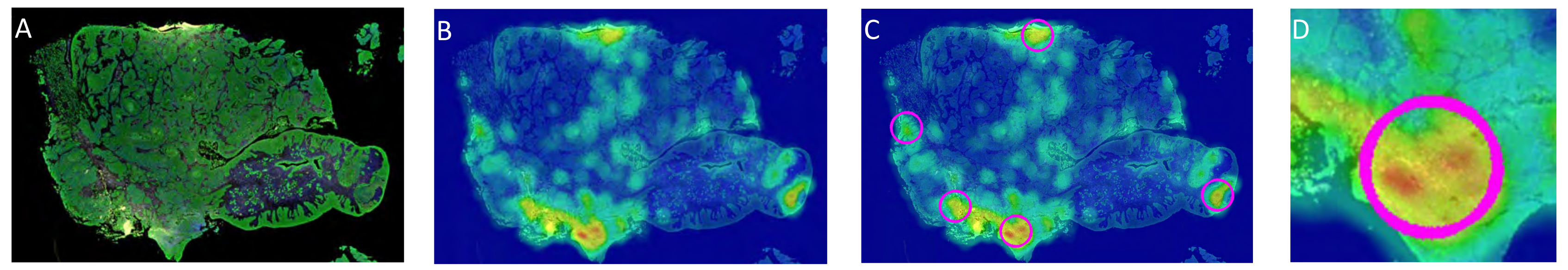

Figure 1: Using automated hotspot detection to select regions of interest (ROIs) for GeoMx. **1A** shows a 4-color GeoMx immunofluorescence (IF) image. For this application, the four colors were Syto13 (nuclear marker, blue), cytokeratin (green), CA-9 (red) and CD3 (yellow). **1B** shows the Visiopharm overlay of a Deep Learning APP trained for tumor segmentation (tumor = blue, stroma = green) . A hotspot analysis was performed for CA-9 within tumor regions, revealing localized CA-9 expression around the edge of the tumor (**1C**) . **1D** shows 4 regions of interest that were chosen based on the CA-9 hotspot analysis. Each of these ROIs can be further analyzed for tumor/stroma (or other marker-based segmentations) to form the areas of illumination (AOIs) that will be collected on GeoMx.

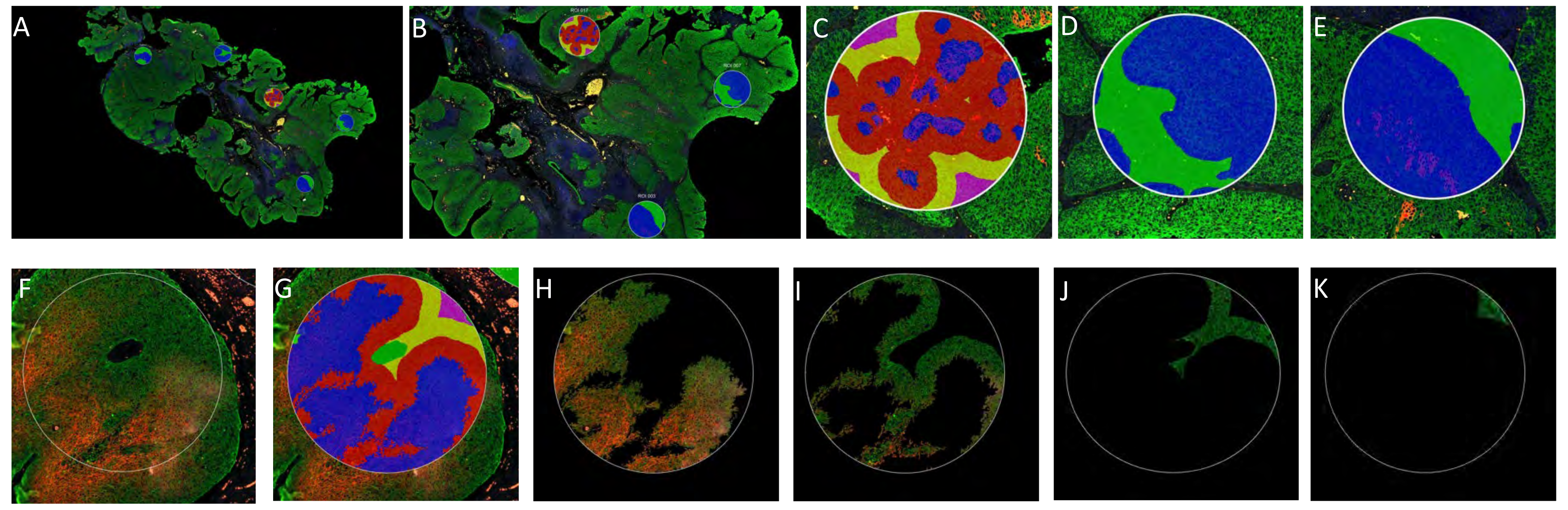

Figure 2: Creating AOIs from CA-9 hotspots using two different methods. **2A** shows a whole-slide 4-color IF images taken on a GeoMx of Sample 16. **2B** shows a zoomed-in portion of the whole slide. For this sample, 7circular hotspots were chosen to be ROIs. These can be seen superimposed on the color IF image. ROIs 17 and 3-7 were segmented using a paint-to-train deep-learning-based approach into tumor and stromal regions (see Figure 4). ROI 2 was created larger than the others, segmented into tumor and stroma, and then the tumor region was segmented into a very high CA-9 expression region and the rest. The high CA-9 region was expanded in 50 μm steps to form concentric regions around the CA-9 hotspot. **2F-2K** shows an expanded view of this process on sample 14 ROI 17 **.**

AI segmentation

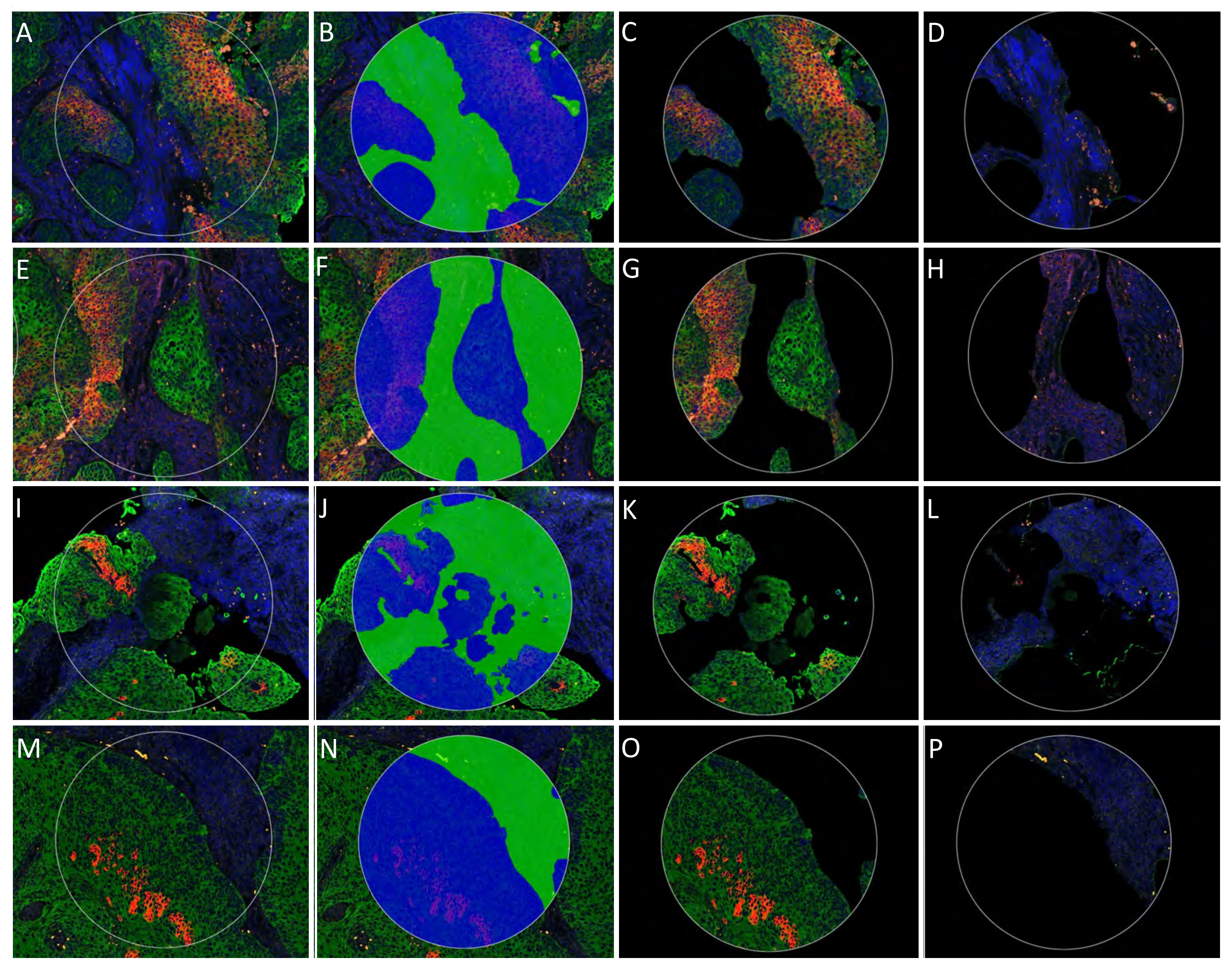

Figure 4: Creation of AOIs based on tumor/stroma tissue segmentation. This is the second method for the generation of AOIs. In this case, each circular ROI was segmented using a paint-to-train deep-learning-based approach into tumor and stromal regions, each of which became an AOI for GeoMx data collection. **4A** - **4D** shows the sequence for ROI 2 of Sample 18. The circular ROI was segmented into tumor (blue) and stroma (green), and each AOI is shown in **4C** (tumor) and **4D** (stroma). Figures **4E** - **4H** show the same sequence of steps for ROI 3 of Sample 18.. Figures **4I-L** and **4M-P** show the same sequence of steps for ROI 4 and ROI 3 of Sample 16.

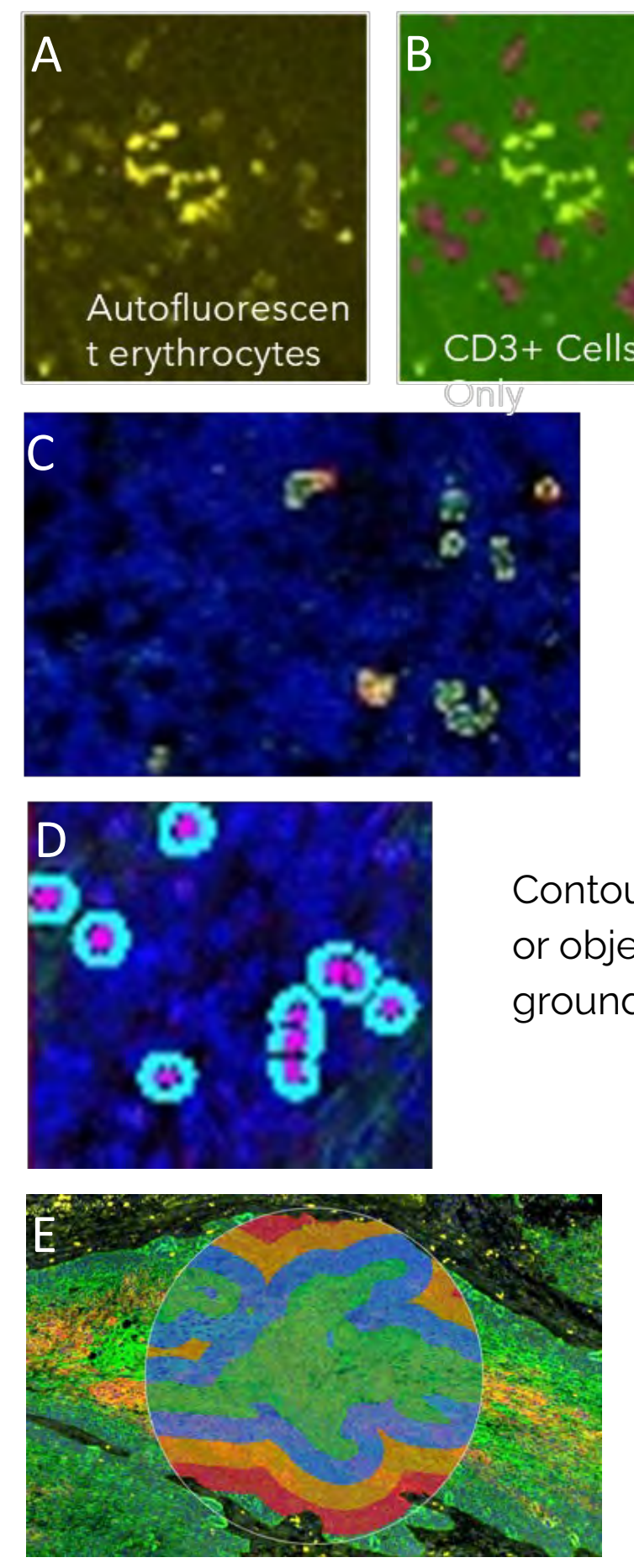

Exclusion of unwanted signals

Segmentation of cells expressing punctate staining patterns, such as RNAscope

Contouring around scattered cells or objects to collect local background signals

Contouring around tissue regions by intensity or distance

Figure 3. Oncotopix AI segmentation unlocks new applications for GeoMx DSP. 3A-D shows a series of other uses of Oncotopix segmentation for GeoMx DSP. The flexibility of trainable deep-learning-based AI means that a wide range of AOIs can be created. **3A-3B** shows the segmentation of cells or tissues using deep learning without interference from tissue autofluorescence, which can be problematic for thresholding methods. **3C** shows finding cells based on punctate RNA stains; one can choose how many spots per cell are to be considered positive. .**3D** shows using contouring to create a penumbra AOI around scattered cells or other objects, to enable the collection of local background signals. **3E** shows using tissue segmentation or hotspot analysis to find a tissue type (in this case hypoxic tissue based on an IF marker) and then contours made around the central area.

Methods: GeoMx DSP together with Oncotopix Discovery

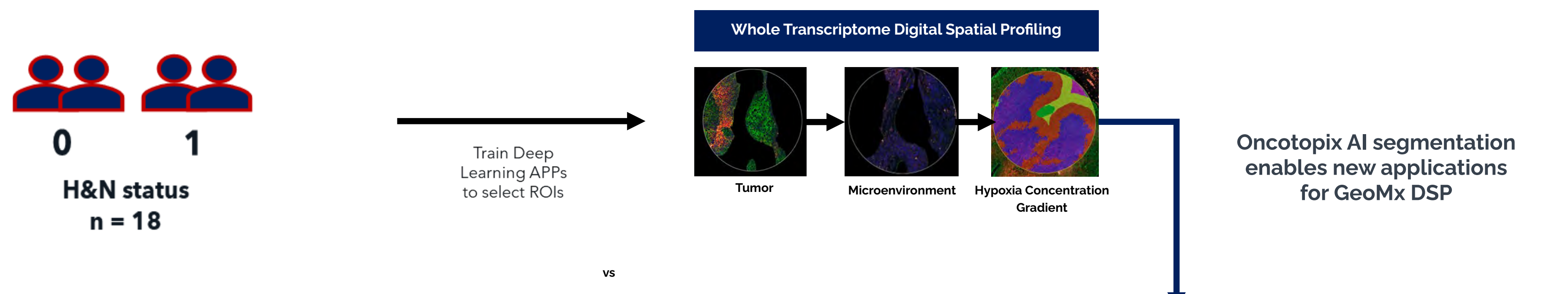

H&N status
n = 18

Train Deep Learning APPs to select ROIs

Whole Transcriptome Digital Spatial Profiling

Oncotopix AI segmentation enables new applications for GeoMx DSP

vs

Sample ID	p16 (1 = pos 0 = neg)	HPV status (1 = pos 0 = neg)	Hypoxia-immune subgroup (from gene signature)	CD3	CA-IX (% tumour cells pos)	PD-L1 tumour (% cells pos)	PD-L1 immune cells	Immune status (from CD3 staining)
1	0	0	Hypoxia^{high}/immune^{low}	low	70	20	low	Immune desert
3	0	0	Hypoxia^{high}/immune^{low}	low	67.5	0	low	Immune desert
5	0	0	Hypoxia^{low}/immune^{high}	high	2.5	17.5	low	Inflamed
9	0	0	Mixed	int	27.5	15	low/high	Inflamed (low)
13	0	0	Hypoxia^{high}/immune^{low}	low	25	0	low	Immune excluded
6	1	0	Mixed	int	35	25	high	Immune excluded
8	1	0	Hypoxia^{low}/immune^{high}	int	10	20	high	Inflamed
10	1	0	Hypoxia^{high}/immune^{low}	low	32.5	0	low	Immune desert
12	1	0	Hypoxia^{high}/immune^{low}	low	10	0	low	Immune desert
15	1	0	Mixed	int	40	0	low	Inflamed (low)
18	1	0	Mixed	high	30	30	high/low	Inflamed
4	0	1	Hypoxia^{low}/immune^{high}	high	20	25	low	Inflamed
11	0	1	Mixed	low	27.5	0	low	Immune excluded
2	1	1	Mixed	high	15	55	low	Immune excluded
7	1	1	Mixed	high	5	32.5	low	Inflamed
14	1	1	Hypoxia^{low}/immune^{high}	high	45	0	low	Inflamed
16	1	1	Hypoxia^{low}/immune^{high}	high	20	15	low	Inflamed
17	1	1	Hypoxia^{low}/immune^{high}	high	2.5	80	high	Inflamed

Figure 1. 18 FFPE blocks from head and neck cohort were used for this study. Details of their HPV-positive and negative status, P16 expression, hypoxia and immune response status were obtained.

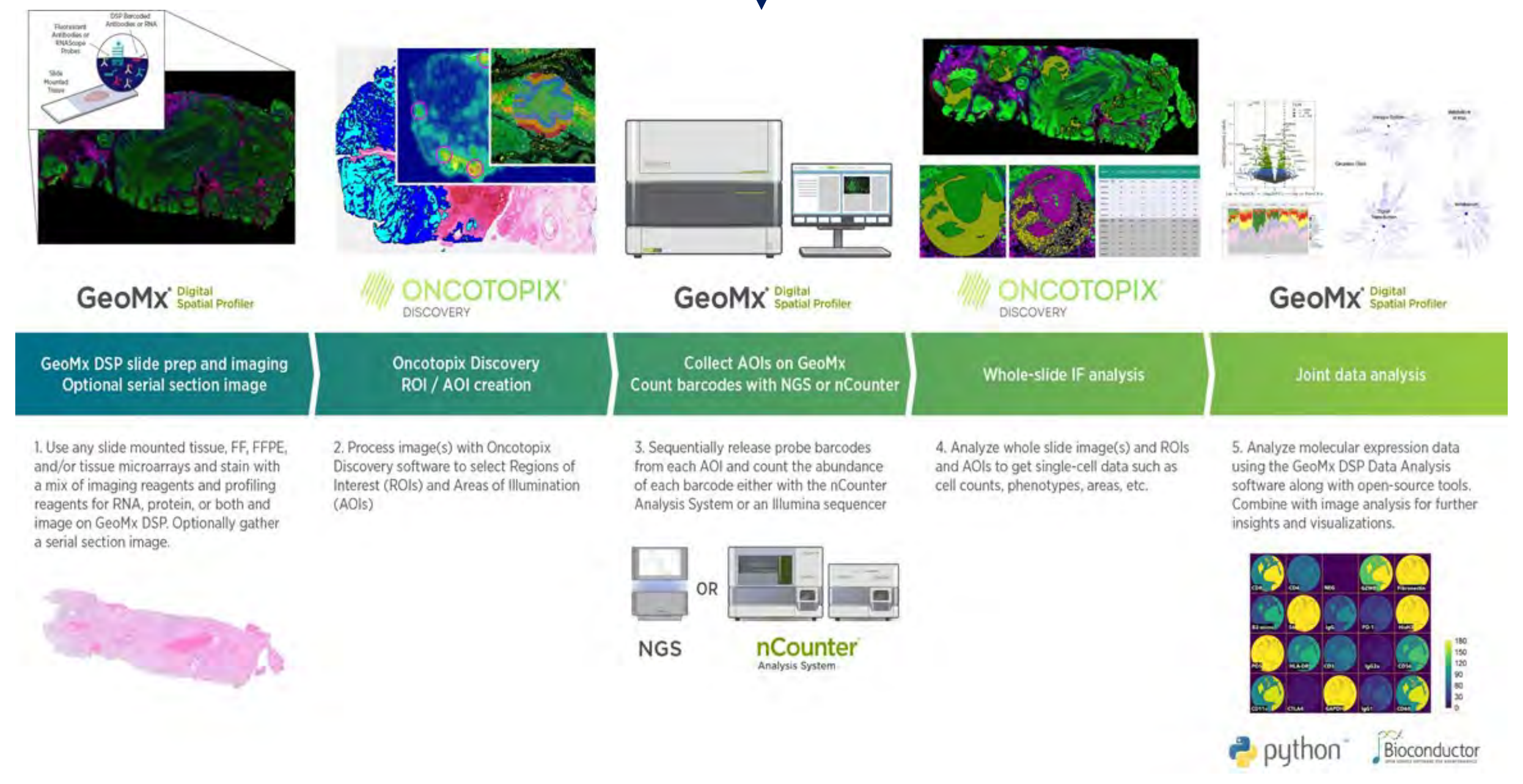

1. GeoMx DSP slide prep and imaging Optional serial section image — Use any slide mounted tissue, FF, FFPE, and/or tissue microarrays and stain with a mix of imaging reagents and profiling reagents for RNA, protein, or both and image on GeoMx DSP. Optionally gather a serial section image.
2. Oncotopix Discovery ROI / AOI creation — Process image(s) with Oncotopix Discovery software to select Regions of Interest (ROIs) and Areas of Illumination (AOIs)
3. Collect AOIs on GeoMx Count barcodes with NGS or nCounter — Sequentially release probe barcodes from each AOI and count the abundance of each barcode either with the nCounter Analysis System or an Illumina sequencer
4. Whole-slide IF analysis — Analyze whole slide image(s) and ROIs and AOIs to get single-cell data such as cell counts, phenotypes, areas, etc.
5. Joint data analysis — Analyze molecular expression data using the GeoMx DSP Data Analysis software along with open-source tools. Combine with image analysis for further insights and visualizations.

Whole Transcriptomics Analysis

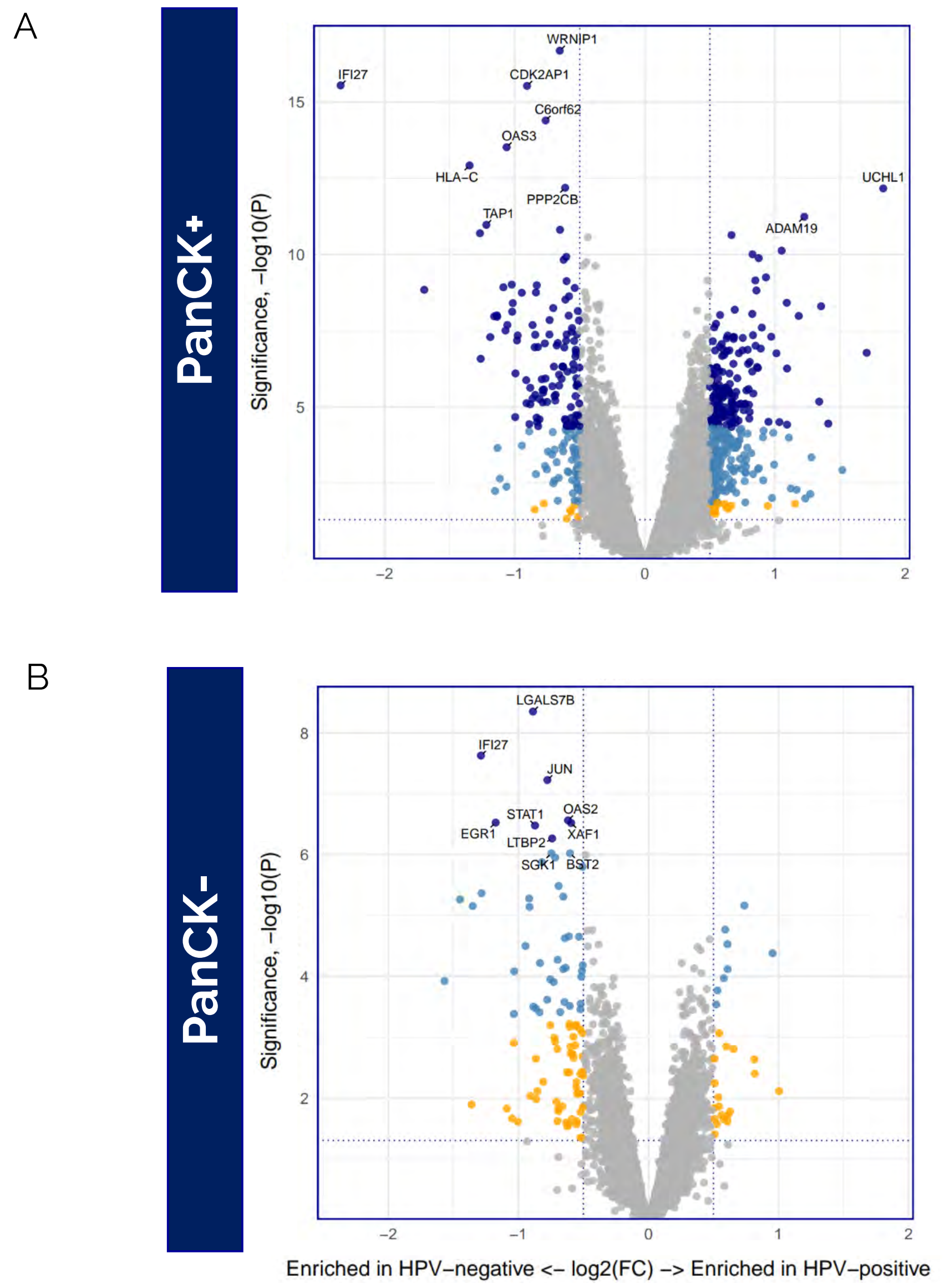

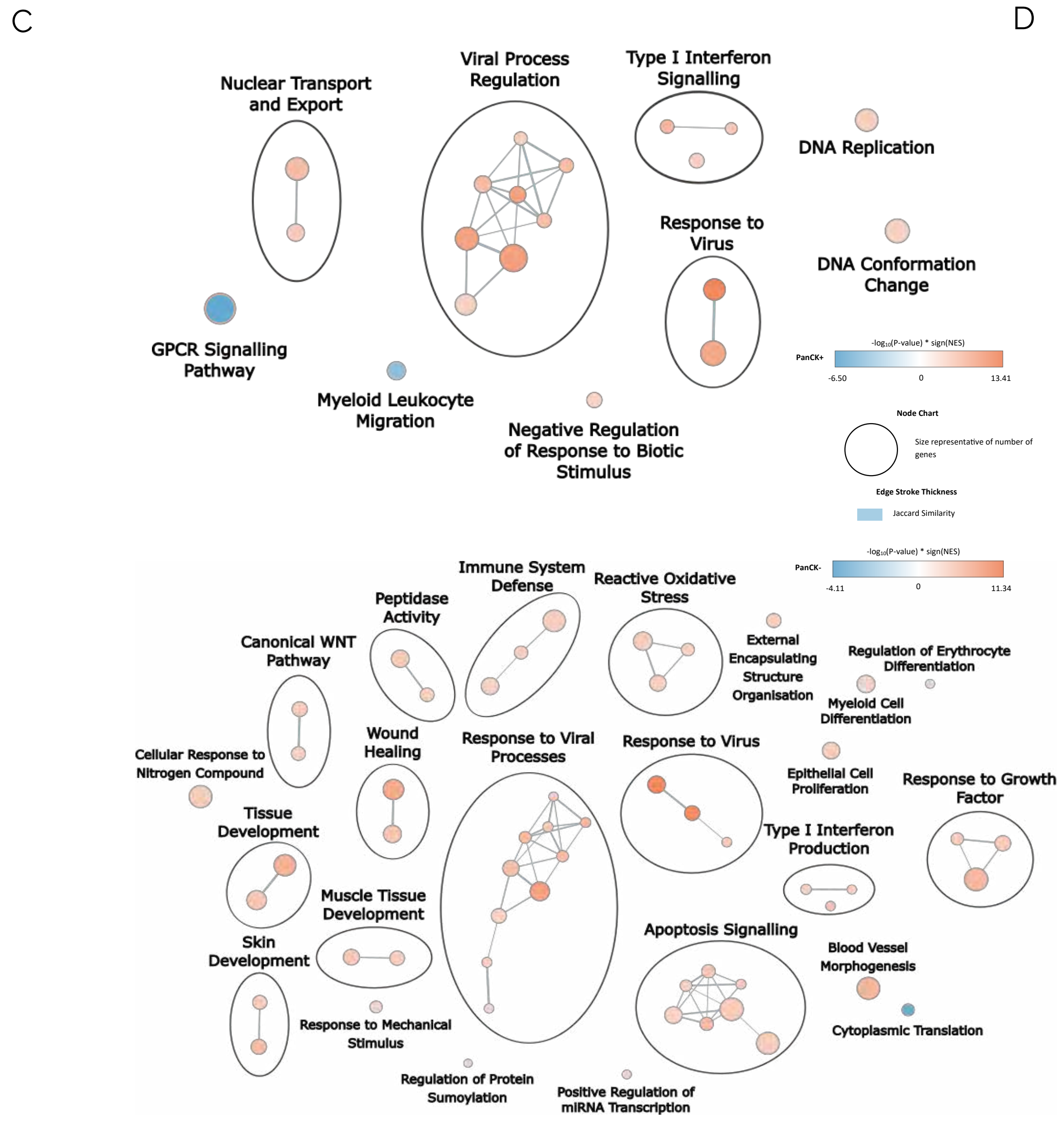

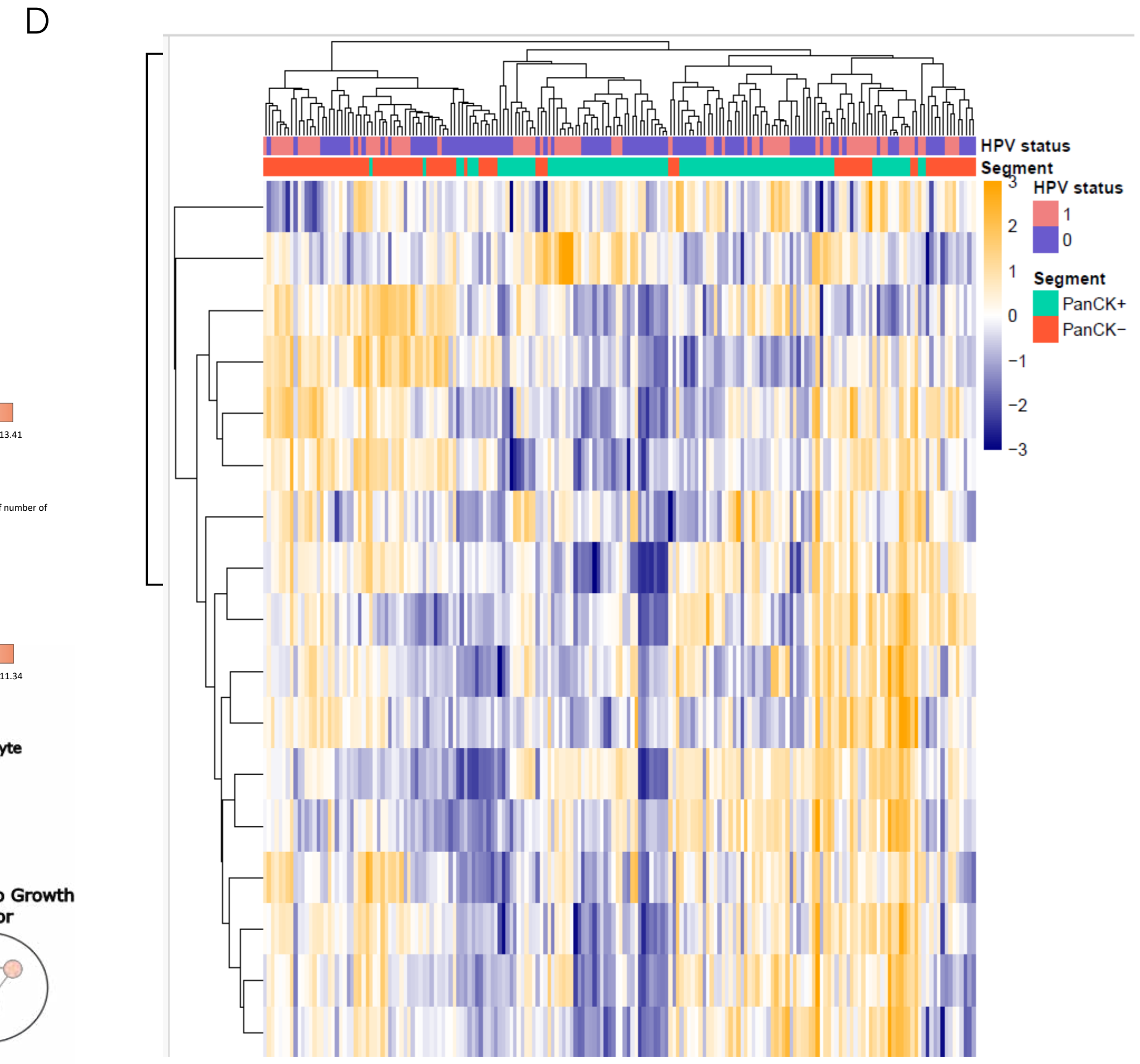

Figure 5: Whole Transcriptome Data Analysis: Whole Transcriptome Data Analysis: 5A and **5B** demonstrate volcano plots for PanCK+ (Top) and PanCK - (bottom) regions. Comparison is across sample with HPV positivity and negativity. The top 10 genes in each setting are highlighted on volcano plots. All genes were ranked according to fold change and adjusted P-value and used as input for Geneset enrichment analysis using the Biological Processes section of the GO database. Significant genesets (FDR < 0.05) are visualised using Cytoscape and the enrichmentMap plugin. **5C)** Each node represents a significant geneset, whereby an increased node size represents more genes. Nodes are colored by a metric combining fold change and p-value to color genesets significantly enriched in HPV-negative samples from white to blue and those significantly enriched in HPV-positive samples from white to red. A more intense blue or red color indicates a more enriched pathway. Nodes connected by lines resemble pathways which have an overlap in genes. The thickness of the line represents the jaccard similarity and can be interpreted as pathways having more genes in common. Pathway groups were initially annotated using the autoAnnotate plugin and subsequently manually reviewed. **5D)** Heatmap of log-transformed, Q3-normalised expression for genes in the 'Response to Type I Interferon' pathway (GO:0034340), scaled by row. Both rows and columns are clustered by average correlation distance. Colour scale indicates low (navy) to high (orange) expression. Samples are annotated for AOI (Segment) and HPV-status.

Multiomics in Visiopharm

Multiomics—MASON

Summary

- **Propath have demonstrated a deployable pipeline, integrating Oncotopix Discovery from Visiopharm and the GeoMx DSP software, leveraging Deep-Learning based image analysis upstream and downstream of the laboratory protocol.**
- **Manual adjustment of any ROIs or AOIs automatically generated in Oncotopix Discovery or GeoMx DSP prior to GeoMx DSP data collection is easy and powerful**
- **Annotation-trained AI/DL AOI segmentation is a significant improvement on traditional threshold-based methods, offering sensitivity, specificity and workflow improvements.**
- **Fully automated ROI and AOI selection are possible for GeoMx DSP using On cotopix Discovery, which can greatly reduce the amount of technician and pathologist time required for large cohort studies**
- **Use of AI to assist in ROI and AOI selection reduces selection bias and time and can increase cellular enrichment for profiling.**
- **Hypoxia signature changes correlated with the contours generated based on hypoxia surrogate IHC marker, validating the spatial concentration gradient methodology**
- **Increasing the cohort from 18 patients confirmed targets of interest from a 6 patient pilot**